Nuclear Engineering and Technology 51 (2019) 2005–2012

Contents lists available at ScienceDirect

Nuclear Engineering and Technology

journal homepage: www.elsevier.com/locate/net

Original Article

Gamma radiation attenuation properties of tellurite glasses: A comparative study

Y. Al-Hadeethi [a, *], M.I. Sayyed [b], S.A. Tijani [a, c]

[a] Department of Physics, Faculty of Science, King Abdulaziz University, Jeddah, 21589, Saudi Arabia
[b] Department of Physics, Faculty of Science, University of Tabuk, Tabuk, Saudi Arabia
[c] Nigerian Nuclear Regulatory Authority, Abuja, Nigeria

ARTICLE INFO

Article history:
Received 6 May 2019
Received in revised form
10 June 2019
Accepted 13 June 2019
Available online 14 June 2019

Keywords:
Tellurite glasses
Gamma radiation
Shielding
Effective atomic number

ABSTRACT

This work investigated the radiation attenuation characteristics of three series of tellurite glass systems with the following compositions: 30PbO-10ZnO-xTeO_2-(60-x)B_2O_3 where x = 10, 30, 40, 50 and 60 mol%, xBaO–xB_2O_3–(100-2x)TeO_2 with x = 15–40 mol% and 50ZnO–(50-x)P_2O_5–xTeO_2, where x = 0, 10, .40 mol%. The results revealed that the attenuation parameters in all the samples decrease with increase in the energy, which implied that all the samples have better interaction with gamma photons at low energies and thus higher photon attenuating efficiency. From the three systems, the samples coded as PbZnBTe60, BaBTe70 and ZnPTe40 have the lowest half value layer values and accordingly have superior photon attenuation efficacy. The maximum effective atomic number values were found for energy less than 0.1 MeV particularly near the K-edges absorption of the heavy atomic number elements such as Te, Ba and Pb. At the lowest energy, the Z_{eff} values are found in the range of 62.33–66.25, 49.43–50.81 and 24.99–35.83 for series 1–3 respectively. Also, we found that the density of the glass remarkably affects the photon attenuation ability of the selected glasses. The mean free path results showed that the PbO-ZnO-TeO_2-B_2O_3 glass system has better radiation shielding efficiency than the glass samples in series 2 and 3.

1. Introduction

Ionizing radiation is popularly used in many applications because of its usefulness in solving many medical and industrial related problems [1–4]. However, its wide usage has led to exposure of personnel and public to its harmful effects which could be deterministic or stochastic. Harmful effects of ionizing radiation is evident [5–8], so protecting the population from these side effects could be achieved by using proper shielding material that can attenuate the ionizing radiation and drastically reduces unwanted radiation exposures.

Glasses are used for radiation shielding purposes mainly because they are usually stable in water and air; transparent to visible light; able to form in large volumes; and ability of having relatively higher densities. Tellurite glass systems are increasingly studied by different researchers due to their superior optical, thermal, structural properties and their potential abilities to form better glasses [9–14]. These glasses are known for their wide spectral region of transparency, corrosion resistant, low melting point; chemical and thermal stability [9,11,12] which are all useful properties considered for radiation shielding materials.

In the literature, different investigations have reported the radiation shielding features of several glass systems [15–21]. However, there are only few works which tried to understand the radiation shielding features of tellurite-based glasses. A summary of previous successful contributions which investigated the radiation shielding properties of tellurite glasses doped with different transition metallic oxides and rare-earth oxides are given as follows.

Ersundu et al. [22] fabricated heavy metal oxides containing TeO_2, MoO_3 and WaO_3; and used the transmission geometry method to report the photon attenuation features for the fabricated samples between 81 and 384 keV. Halimah et al. [23] also studied the effects of Bi_2O_3 on the gamma ray shielding ability of boro-tellurite glass. They prepared seven boro-tellurite glass samples with different amount of Bi_2O_3 (varying from 0 to 30 mol%) by melt quenching method. The authors reported that the sample with

* Corresponding author.
E-mail addresses: yalhadeethi@kau.edu.sa (Y. Al-Hadeethi), mabualssayed@ut.edu.sa (M.I. Sayyed).

https://doi.org/10.1016/j.net.2019.06.014

30 mol% of bismuth oxide had the lowest mean free path and thus had superior radiation attenuation properties. In addition, Sayyed [24] assessed the photon shielding performance of tellurite glasses with some oxides such as PbO, MgO, BaO and ZnO using both the WinXCom program and the G-P method. He discovered that the glass sample with the composition −80 TeO_2-20PbO- had the lowest half value layer. Tekin et al. [25] simulated the mass attenuation coefficients for borate silicate tellurite glasses with different Bi_2O_3 content using Monte Carlo simulation. The simulated results were compared with the theoretical data evaluated by XCOM.

Gaikwad et al. [26] reported the effect of PbO on the photon shielding features of PbO-TeO_2-WO_3 glass system and they compared the shielding parameters of this system with some reference materials such as commercial glasses and other glass systems from the literature. The authors concluded that this glass system could be developed as shielding protection glasses because of its high density and high value of the attenuation coefficient parameters. In another work, Sayyed et al. [27] utilized the G-P fitting approach to evaluate the buildup factors for TeO_2-WO_3 glass system and found that this glass system is appropriate for shielding applications. Increasing the WO_3 content of this glass system improved the ability of the sample to reduce the intensity of gamma photons. Recently, Vani et al. [28] prepared five tellurite glass samples with different content of ZnF_2 and BaF_2; and investigated the radiation shielding effectiveness for these samples using XCOM software. The results demonstrated that the presence of more BaF_2 content in the glass sample can enhance the shielding performance of the sample and thus the glass could be used as replacement for the traditional shielding materials such as concrete.

In this work, we are motivated by the few works that reported the radiation shielding abilities of tellurite-based glasses to further extend the existing work so that a better understanding of ionizing radiation interaction with tellurite-based glass systems could be achieved. Along these lines, we have theoretically investigated the radiation shielding characteristics of three tellurite-based glass systems.

2. Materials and method

This work aimed to report the photon shielding parameters of some tellurite glasses. Three glass systems were selected for this purpose and the necessary properties of these glasses were summarized in Table 1. The first series was 30PbO-10ZnO-xTeO_2-(60-x)B_2O_3 (where x = 10, 30, 40, 50 and 60 mol%) and the samples in this series have the following codes: “PbZnBTe10”, “PbZnBTe30”, “PbZnBTe40”, “PbZnBTe50”, “and “PbZnBTe60”. The second series was xBaO–xB_2O_3–(100-2x)TeO_2 (with x = 15–40 mol%) and the glasses in series 2 have their codes as: “BaBTe20”, “BaBTe30”, “BaBTe40”, “BaBTe50”, “BaBTe60” and “BaBTe70”. The third series was 50ZnO–(50-x)P_2O_5–xTeO_2 (where x = 0, 10, ….40 mol%) and the samples were coded as: “ZnPTe0”, “ZnPTe10”, “ZnPTe20”, “ZnPTe30” and “ZnPTe40”. The densities of the glasses in series 1, 2 and 3 were adopted from Refs. [29–31]. Many shielding parameters are used to assess the change in the photons’ intensity through materials by scattering or absorption. One of these parameters is the linear attenuation coefficient (μ) which explains the fraction of photons which is scattered or absorbed per unit thickness of the sample. This attenuation parameter is related to another parameter known as the mass attenuation coefficient (μ/ρ) which describes how easily certain materials could be penetrated by gamma photons [32]. Higher μ/ρ values for a certain specimen indicate more photons interaction with it and thus fewer photons can penetrate the sample. The μ/ρ values for several elements (for Z ≤ 100) are readily available in WinXcom software [33]. Therefore, for any glass sample, we can use the additive rule to evaluate its μ/ρ by equation (1) [21].

$$(\mu/\rho)_{glass} = \Sigma w_i(\mu/\rho)_i \quad (1)$$

where w_i denotes the weight fraction of the elements in the sample. For the present tellurite glasses, we evaluated the μ/ρ for energy varying from 15 keV to 15 MeV.

The effective atomic number (Z_{eff}) is a common parameter for examining gamma photons interaction for a material composed of different elements (say glassy system for example). It is important to state that the higher values of Z_{eff} for the glass sample, the greater will be the number of photons absorbed by the glass sample [34].

Half value layer (HVL) is another quantity which gives an indication about the effectiveness of a sample to attenuate photons. HVL is the thickness of the attenuator required to absorb half of the initial intensity of the photons. The mean free path (MFP) is an interesting property in terms of gamma ray protection. The MFP of any sample describes its gamma ray attenuation strength. Both parameters were calculated using the following relations [28]:

$$HVL = 0.693/\mu \quad (2)$$

$$MFP = 1/\mu \quad (3)$$

Table 1
The chemical composition and density of the selected tellurite glasses.

Glass code	Glass composition	Density gm/cm^3	Reference
series 1			
PbZnBTe10	30PbO-10ZnO-10TeO_2-50B_2O_3	4.98	[29]
PbZnBTe30	30PbO-10ZnO-30TeO_2-30B_2O_3	5.55	[29]
PbZnBTe40	30PbO-10ZnO-40TeO_2-20B_2O_3	5.92	[29]
PbZnBTe50	30PbO-10ZnO-50TeO_2-10B_2O_3	6.22	[29]
PbZnBTe60	30PbO-10ZnO-60TeO_2-0B_2O_3	6.55	[29]
series 2			
BaBTe20	40BaO-40B_2O_3-20TeO_2	4.17	[30]
BaBTe30	35BaO-35B_2O_3-30TeO_2	4.21	[30]
BaBTe40	30BaO-30B_2O_3-40TeO_2	4.33	[30]
BaBTe50	25BaO-25B_2O_3-50TeO_2	4.37	[30]
BaBTe60	20BaO-20B_2O_3-60TeO_2	4.54	[30]
BaBTe70	15BaO-15B_2O_3-70TeO_2	4.86	[30]
series 3			
ZnPTe0	50ZnO-50P_2O_5-0TeO_2	2.84	[31]
ZnPTe10	50ZnO-40P_2O_5-10TeO_2	3.34	[31]
ZnPTe20	50ZnO-30P_2O_5-20TeO_2	3.86	[31]
ZnPTe30	50ZnO-20P_2O_5-30TeO_2	4.38	[31]
ZnPTe40	50ZnO-10P_2O_5-40TeO_2	4.85	[31]

3. Results and discussion

Figs. 1–3 show the variation of μ/ρ for the selected glass series at several energies varying from 15 keV to 15 MeV. The trend in μ/ρ observed in these figures is similar to some earlier works on some glass systems (e.g lead glasses) [35], and bismuth borate glasses [36].

As can be seen in Figs. 1–3, the μ/ρ has a very high value initially (i.e. at 15 keV) and then shows a decrease in trend with increasing the energy. At 15 keV, the μ/ρ lies within the range of 64.9–66.7 cm^2/g, 40.1–40.7 cm^2/g and 35.6–45.3 cm^2/g for PbO-ZnO-TeO_2-B_2O_3, BaO-B_2O_3- TeO_2 and ZnO-P_2O_5- TeO_2 glass systems respectively. These high values in μ/ρ at low energy is understandable with the fact that the photoelectric mechanism is dominating, and this mechanism appears clearly at the low photon

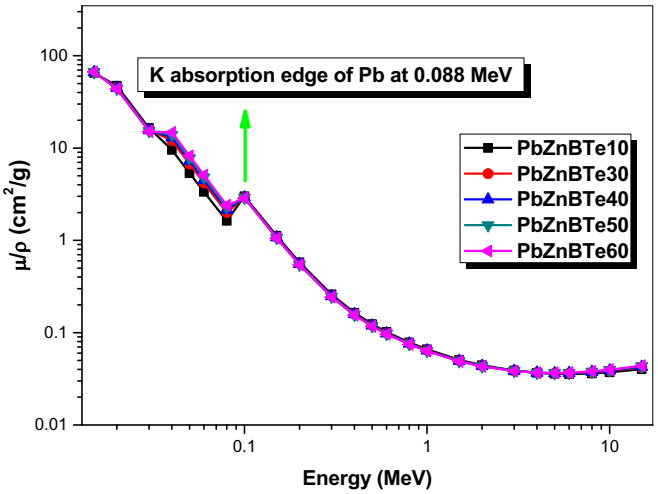

Fig. 1. The mass attenuation coefficient (cm^2/g) for the PbO-ZnO-TeO_2-B_2O_3 glass system.

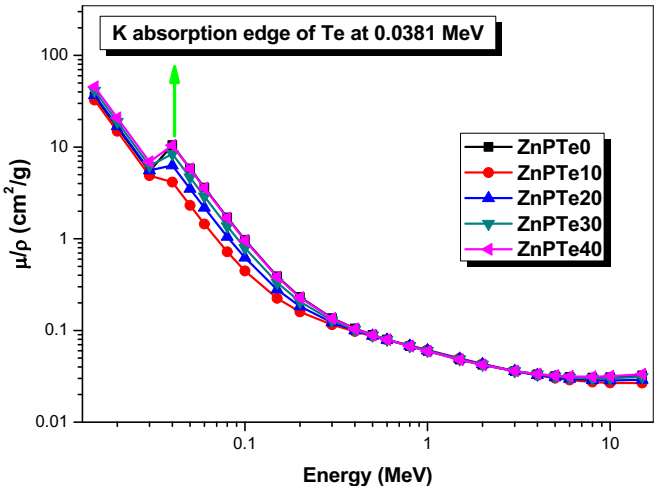

Fig. 3. The mass attenuation coefficient (cm^2/g) for the ZnO-P_2O_5-TeO_2 glass system.

energies. The cross section of this process varies with the atomic number as Z^{4-5}, and the selected glasses contain elements with high atomic number (i.e. Te in the three series, Pb in series 1 and Ba in series 2) which increases the probability of photoelectric interaction to occur. Also, different jumps in μ/ρ at low energy can be seen from Figs. 1–3. The jump in Fig. 1 appears at 0.1 MeV (in the vicinity of the K-absorption edge of lead), while in Fig. 2 it occurs at 0.04 MeV (corresponding to the K-absorption edge of both elements with atomic numbers 56 and 52, namely Ba and Te respectively) and in Fig. 3 also it occurs at 0.04 MeV due to the K-absorption edge of Te. The results show that the μ/ρ values are increasing with the addition of TeO_2 in the three glass series. In series 1, the replacement of B_2O_3 by TeO_2 causes the increasing in the μ/ρ values. In series 2, since the Ba and Te have close atomic numbers (56 and 52 respectively), so a slight increment (unnoticeable) in this parameter is observed in Fig. 2. In series 3, both ZnO and P_2O_5 contents are decreasing while TeO_2 content is increased and it is known that TeO_2 has higher attenuation coefficient than both ZnO and P_2O_5; and this explains the increasing μ/ρ values observed in Fig. 3. At high energy zone, the μ/ρ values for the three series are very small (in order of 0.044 cm^2/g for series1, 0.036 cm^2/g for series 2 and 0.032 cm^2/g for series 3). This implies that the glass sample can attenuate the photons effectively at low energies and as the photons energy increase, the ability of the selected samples to block the photons decrease, thus high energy photons can move and transmit through the samples. Among the present glasses, PbZnBTe60 (from series 1), BaBTe70 (from series 2) and ZnPTe40 (from series 3) have the highest μ/ρ values. These three samples are compared with two different commercial window glasses (type A and type B) in terms of μ/ρ as shown in Fig. 4. The compositions of these window glasses were taken from

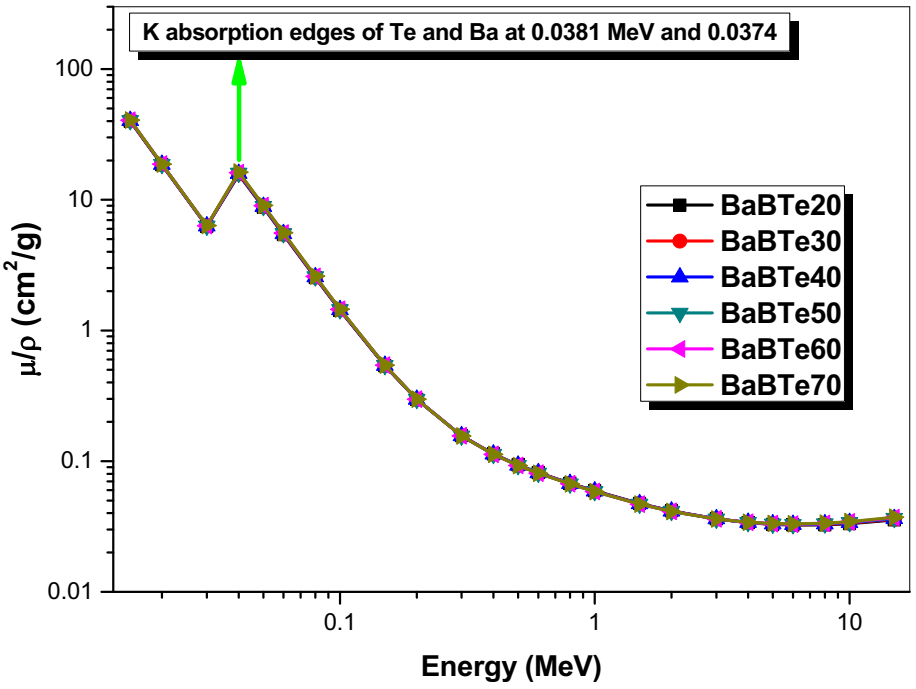

Fig. 2. The mass attenuation coefficient (cm^2/g) for the BaO-B_2O_3-TeO_2 glass system.

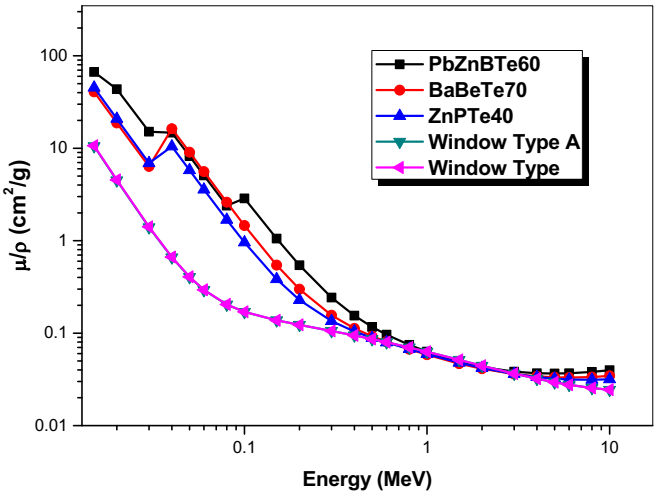

Fig. 4. The mass attenuation coefficient (cm^2/g) for PbZnBTe60, BaBeTe70, ZnPTe40 glasses in comparison with two window glasses.

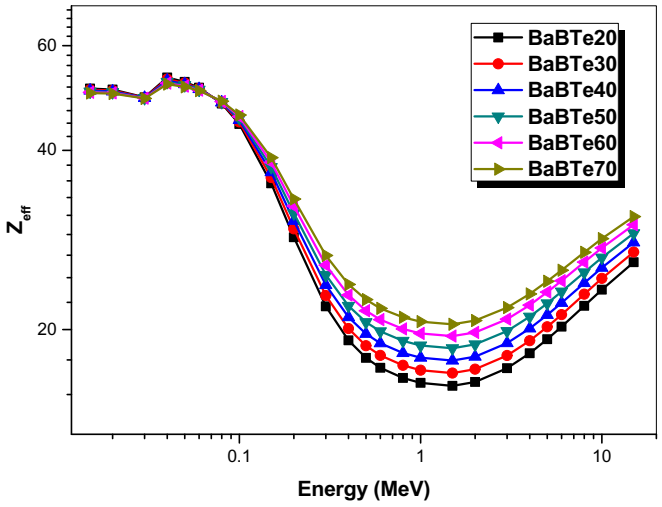

Fig. 6. The effective atomic number for the BaO-B_2O_3-TeO_2 glass system.

Ref. [37]. The results in this curve showed that PbZnBTe60, BaBTe70 and ZnPTe40 glasses have higher μ/ρ values than the window glasses type A and B, also PbZnBTe60 has higher μ/ρ values than BaBTe70 and ZnPTe40 samples since this sample contains 30 mol% of PbO and 60 mol% of TeO_2.

From this parameter given in Figs. 1–3, we calculated the Z_{eff} for the glass systems under examination and we presented the obtained results in Figs. 5–7 for PbO-ZnO-TeO_2-B_2O_3, BaO–B_2O_3–TeO_2 and ZnO–P_2O_5–TeO_2 glass systems respectively.

The present Z_{eff} curves for the investigated samples have similar trend with the results obtained by Bagheria et al. [38] who studied

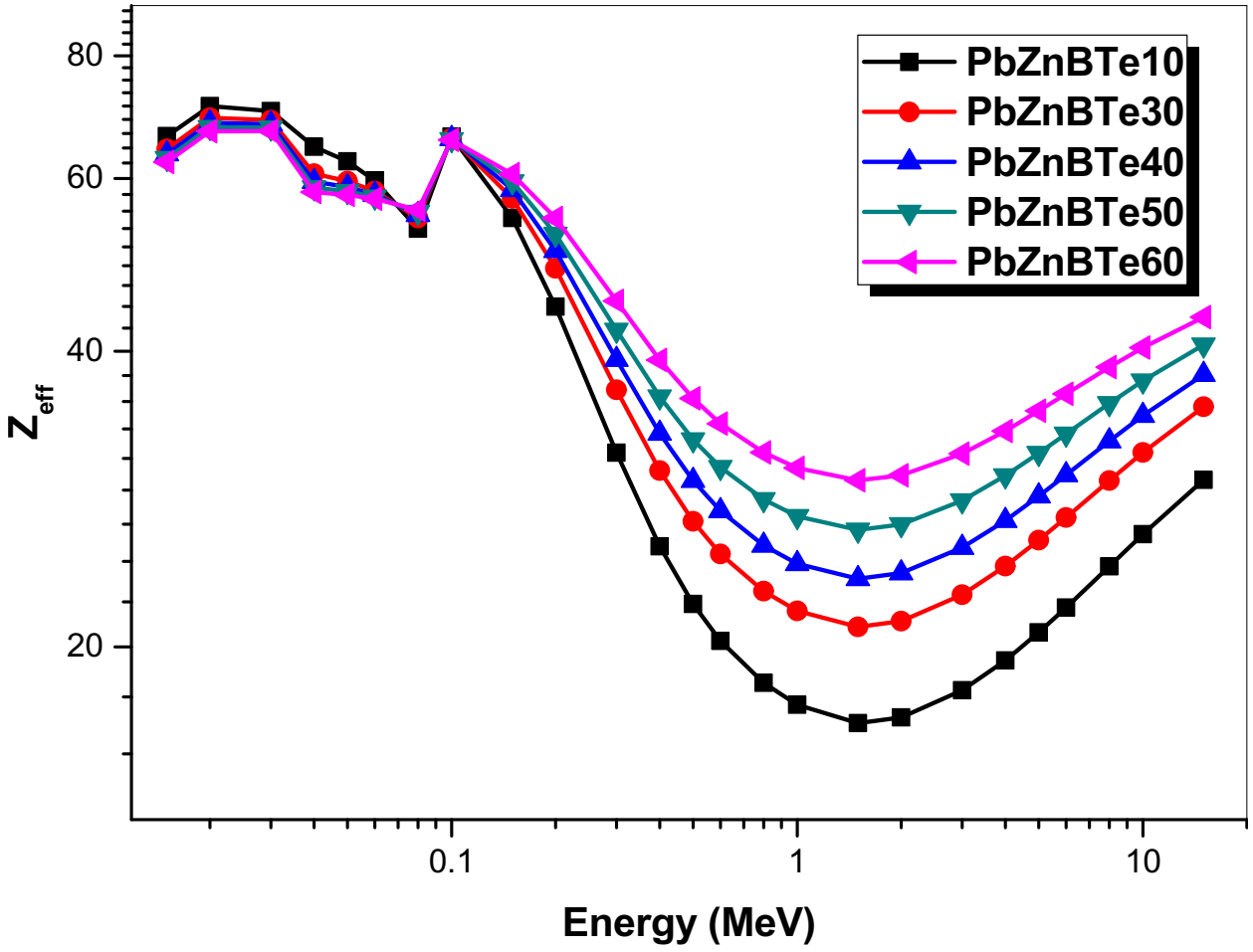

Fig. 5. The effective atomic number for the PbO-ZnO-TeO_2-B_2O_3 glass system.

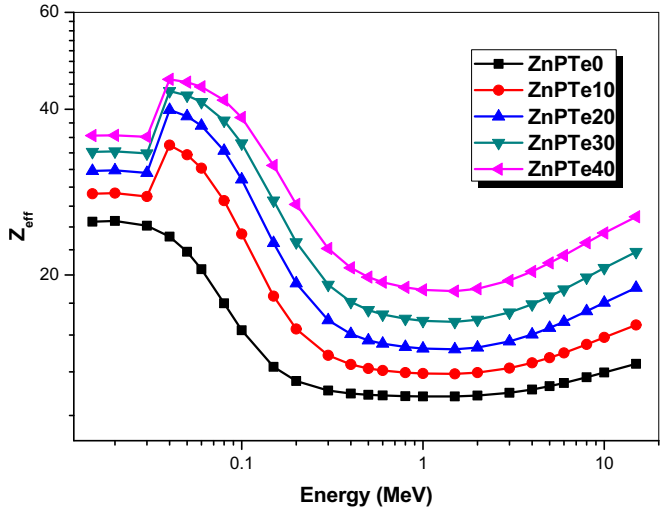

Fig. 7. The effective atomic number for the ZnO-P_2O_5-TeO_2 glass system.

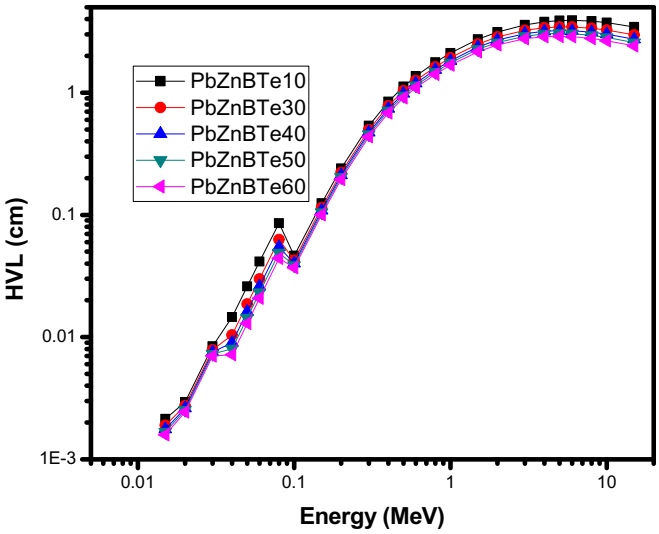

Fig. 8. The half value layer (cm) for the PbO-ZnO-TeO_2-B_2O_3 glass system.

the photon attenuation ability of silicate glass system containing various contents of heavy metal oxides.

Evidently, Z_{eff} attains maximum values for the glass samples in series 1–3 when E < 0.1 MeV (which is known as photoelectric region), particularly near the K-edges absorption of Te in Figs. 5–7 as well as the K-edges of Pb (in Fig. 5), and Ba (in Fig. 6). At the lowest energy, the Z_{eff} values are found in the range of 62.33–66.25, 49.43–50.81 and 24.99–35.83 for series 1–3 respectively. The high Z_{eff} values for the present glasses (especially the glasses in series 1 and series 2) could be attributed to the high Z elements (Pb in the first series and Ba in the second series, in addition to Te in all samples) and the radiation physics concepts postulated that the cross section of the photoelectric process (which is important process for E < 0.1 MeV) depends highly on the atomic number (as Z^{4-5}), thus we observed the high Z_{eff} values at very low energy.

As it could be noticed from Figs. 5–7, for 0.4 MeV < E < 3 MeV where Compton scattering mechanism is the fundamental mechanism, the variation in Z_{eff} with the energy is negligible and minimum Z_{eff} values could be seen between these energies. While, for E > 3 MeV, this parameter showed an increase in trend with further increase in the energy. This can be explained according to the pair production process as discussed recently by Wilson [20]. The addition of TeO_2 leads to increase in the Z_{eff} values in the first series and we can see that PbZnBTe10 and PbZnBTe60 have the lowest and highest Z_{eff} respectively (Fig. 5). From Figs. 6 and 7, the increment of TeO_2 from 20 to 70 mol% in the second series and from 0 to 40 mol% in the third series also leads to increase in the Z_{eff}. This trend in Z_{eff} is primarily due to the high atomic number of Te (Z = 52) when compared to B (in series 1 and 2), P and Zn in series 3. From this result we can conclude that to obtain a glass specimen which has superior photon attenuation efficiency, a large concentration of TeO_2 must be used. Additionally, the data presented in Figs. 5–7 revealed that the Z_{eff} for the glasses in series 1 are higher than the corresponding values in series 2 and 3, while the glasses in series 3 are the lowest. The high Z_{eff} values for PbZnBTe10-60 glasses are due to the presence of Pb and Te because of their high atomic numbers. It is reported that the sample which possesses high Z_{eff} can effectively shield gamma photons [15], consequently we can say that the PbO-ZnO-TeO_2–B_2O_3 glass system has better radiation shielding efficiency than the glass samples in series 2 and 3. As a summary of the Z_{eff} curves, we can state that, in order to enhance the photon absorption capability of the selected samples, high atomic number elements (such as Pb, Ba … etc) in an

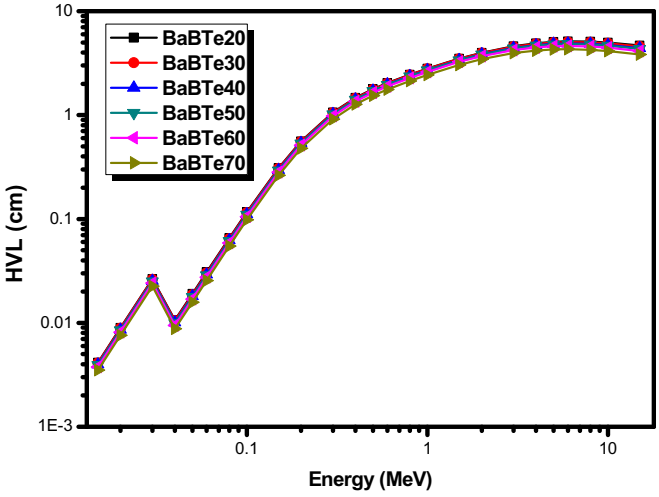

Fig. 9. The half value layer (cm) for the BaO-B_2O_3-TeO_2 glass system.

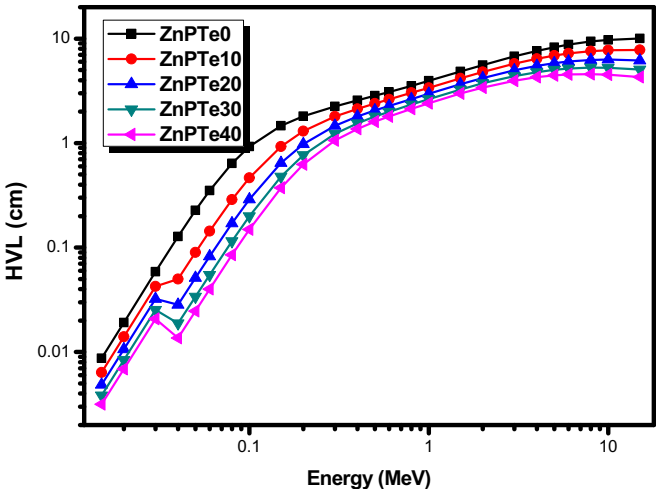

Fig. 10. The half value layer (cm) for the ZnO-P_2O_5-TeO_2 glass system.

appropriate fraction must be utilized during glass formation process.

The HVL curves for the three series of glasses are shown in Figs. 8–10. As it is clear from these curves, the values of HVL for the PbO-ZnO-TeO_2-B_2O_3, BaO-B_2O_3-TeO_2 and ZnO-P_2O_5-TeO_2 glasses are nearly constant between 0.015 and 0.1 MeV and are in order of 0.0016–0.0021 cm for series 1, 0.0035–0.0042 cm for series 2 and 0.0032–0.0087 cm for series 3 at 15 keV. Also the lowest HVL values are observed between 0.015 and 0.1 MeV (low energy zone) and this means that the probability of interaction of low energy photons with the glass samples is very high, so small thickness of the sample can attenuate or block the photons in penetrating through the sample. Beyond 0.1 MeV, as it could be observed from the HVL curves, this parameter highly depends on the energy, where increasing the energy results in the increased in the HVL for all samples presented in Figs. 8–10, and this is predictable findings based on the μ/ρ curves given in Figs. 1–3. The present behavior of HVL for the three series can be attributed to the photon-matter interaction mechanisms as described for the μ/ρ.

It is worthwhile to state that the higher HVL strongly suggests more distance that the photons will travel within the glass specimen. For this reason, in the practical applications we try to prepare glass sample with a potential of having low HVL, so that the sample could have better ability to attenuate the incoming radiation [39].

Examining the data exhibited in Figs. 8–10, it is clear that HVL decreases with the addition of TeO_2 in the glasses in series 1 (Fig. 8), and the sample coded as PbZnBTe60 has the lowest HVL. In series 2 (Fig. 9), as the concentration of TeO_2 increases, the HVL decreases which shows the probability of gamma photon interaction with the BaBTe20-BaBTe70 samples is high at higher TeO_2 concentration. For the glasses presented in Fig. 10, the HVL also decreases when ZnO and P_2O_5 are replaced by TeO_2. The highest HVL is corresponding to the sample with 50 mol% of ZnO and P_2O_5. The reason for the decrement of HVL with the addition of TeO_2 for the three glass systems could be described with the following: increase in the TeO_2 content led to increase in the density of the sample (see Table 1). This increases the probability of interaction between the photon and the glass sample, so fewer photons can penetrate the glass sample. In other words, the density of the glass remarkably affects the photon attenuation ability of the selected glass systems. In addition, the results presented in Figs. 8–10 demonstrated that the HVL values of PbO-ZnO-TeO_2-B_2O_3 glass samples (i.e. series 1) are lower than the HVL of the glasses in series 2 and series 3. This is because each sample in series 1 contains 30 mol% of PbO and it is known that lead can effectively attenuate the gamma photons since Pb has high atomic number and high density, so it is very suitable for blocking the incoming photons. This result emphasizes that PbO-ZnO-TeO_2-B_2O_3 glass system has better photon absorption capacity in comparison to the glasses in series 2 and 3.

Figs. 11–13 show a comparison of MFP for the glasses in series 1–3 with ordinary concrete and steel-magnetite [40]; and two commercial shielding glasses RS-360 and RS-520 [41]. From Fig. 11, the MFP for the PbO-ZnO-TeO_2-B_2O_3 glass system is lower than the MFP of ordinary concrete, steel magnetite and RS-360 which implies that all the glass samples in the first series have better attenuation performance than the two types of concrete used for comparison and RS-360 glass. From the same figure, the MFP of RS-520 is comparable to the MFP of PbZnBTe30 and higher than PbZnBTe40- PbZnBTe60 glasses.

It can be seen from Fig. 12 that all glass samples in series 2 have lower MFP than ordinary concrete, steel magnetite and RS-360. Meanwhile, the MFP of the RS-520 is lower than the HVL of the glasses in series 2. The results presented in Fig. 13 show that the MFP values of all glasses in series 3 are lower than those of ordinary concrete, the MFP values of steel magnetite are slightly lower than

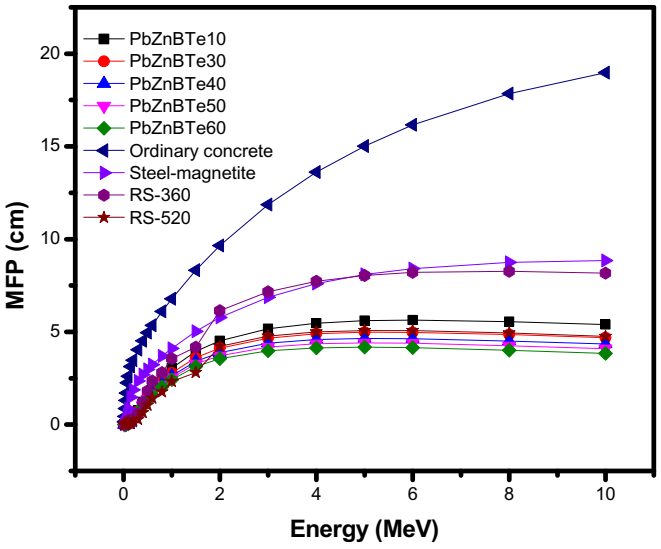

Fig. 11. The mean free path (cm) for the PbO-ZnO-TeO_2-B_2O_3 glass system in comparison with some concretes and shielding glasses.

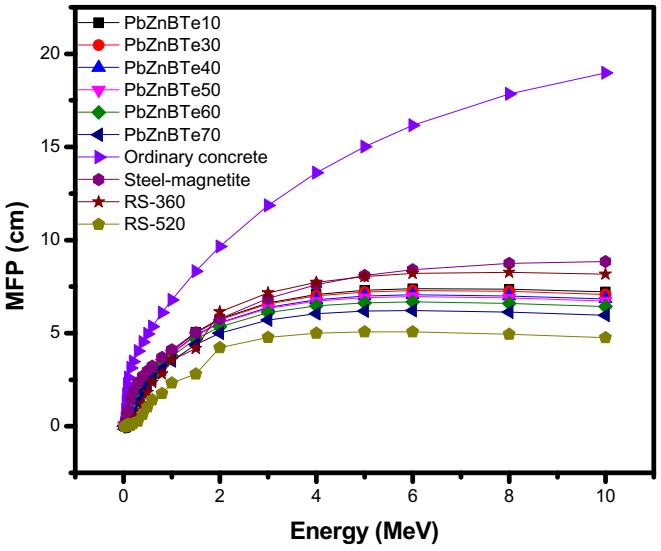

Fig. 12. The mean free path (cm) for the BaO-B_2O_3-TeO_2 glass system in comparison with some concretes and shielding glasses.

ZnPTe20 while higher than the MFP of ZnPTe30 and ZnPTe40 glasses. Also, from the same figure, RS-360 has lower MFP than ZnPTe30 and ZnPTe40 glasses, while RS-520 has lower MFP than all samples in series 3. From Figs. 11–13 we can state that the selected systems have comparable or better shielding characteristics than some concretes and commercial glasses used for the radiation protection applications.

4. Conclusion

In the present work, we reported different radiation shielding parameters for three tellurite based glass systems. The μ/ρ values were found to decrease with increase in energy, so the glass sample can attenuate the photons effectively at low energies. The results revealed that the μ/ρ values are increasing with the addition of TeO_2 in the three selected glass systems. The PbZnBTe60 (from series 1), BaBTe70 (from series 2) and ZnPTe40 (from series 3) glasses have

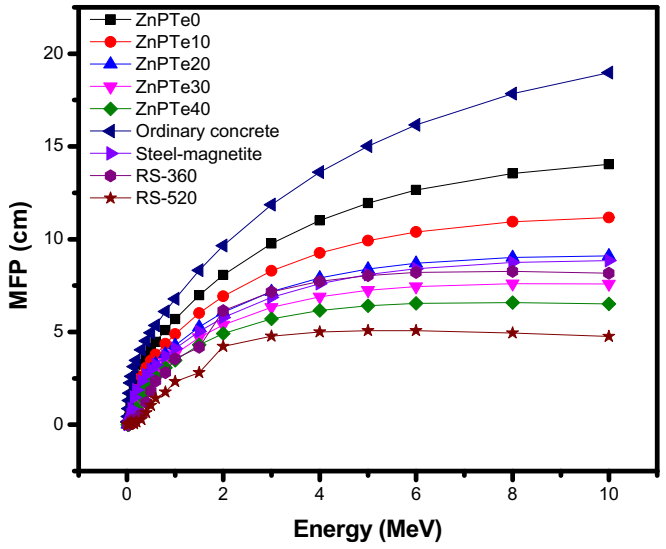

Fig. 13. The mean free path (cm) for the ZnO-P_2O_5-TeO_2 glass system in comparison with some concretes and shielding glasses.

the lowest HVL and MFP values so they have superior radiation shielding effectiveness. At 15 keV, the Z_{eff} values were in the range of 62.33–66.25, 49.43–50.81 and 24.99–35.83 for series 1–3 respectively. From HVL figures, we found that the density of the glass remarkably affects the photon attenuation ability of the selected glass systems. The mean free path results showed that the PbO-ZnO-TeO_2–B_2O_3 glass system (series 1) had a better radiation shielding efficiency than the glass samples in series 2 and 3. The MFP results revealed that the selected Te-based glass systems have comparable or better shielding characteristics than some concretes and commercial glasses used for the radiation protection applications. The present glass systems are capable to efficiently withstand the potential hazardous ionizing radiation harms for human beings also further extending their applications in industrial sectors.

Acknowledgment

This work was supported by the Deanship of Scientific Research (DSR), King Abdulaziz University, Jeddah, under grant No. (D-130-130-1440). The authors, therefore, gratefully acknowledge the DSR technical and financial support.

References

[1] Ashok Kumar, Gamma ray shielding properties of PbO-Li_2O-B_2O_3 glasses, Radiat. Phys. Chem. 136 (2017) 50–53.
[2] M.G. Dong, O. Agar, H.O. Tekin, O. Kilicoglu, Kawa M. Kaky, M.I. Sayyed, A comparative study on gamma photon shielding features of various germanate glass systems, Composites Part B 165 (2019) 636–647.
[3] Erdem Şakar, Uğur Akbaba, Eugeniusz Zukowski, Gürol Ali, Gamma and neutron radiation effect on Compton profile of the multi-walled carbon nanotubes, Nucl. Instrum. Methods Phys. Res. Sect. B Beam Interact. Mater. Atoms 437 (2018) 20–26.
[4] S.S. Obaid, M.I. Sayyed, D.K. Gaikwad, H.O. Tekin, Y. Elmahroug, P.P. Pawar, Photon attenuation coefficients of different rock samples using MCNPX Geant4 simulation codes and experimental results: a comparison study, Radiat. Eff. Defect Solid (2018) 1–15.
[5] P.M. Williams, S. Fletcher, Health effects of prenatal radiation exposure - American family physician, Am. Fam. Physician (2010). http://www.aafp.org/afp/2010/0901/p488.html#sec-2.
[6] Erdem Şakar, Mehmet Büyükyıldız, Bünyamin Alım, Betül Ceviz Şakar, Murat Kurudirek, Leaded brass alloys for gamma-ray shielding applications, Radiat. Phys. Chem. 159 (2019) 64–69.
[7] F. Akman, I.H. Geçibesler, M.I. Sayyed, S.A. Tijani, A.R. Tufekci, I. Demirtas, Determination of some useful radiation interaction parameters for waste foods, Nuclear Eng. Technol. 50 (2018) 944–949.
[8] F. Akman, R. Durak, M.F. Turhan, M.R. Kaçal, Studies on effective atomic numbers, electron densities from mass attenuation coefficients near the K edge in some samarium compounds, Appl. Radiat. Isot. 101 (2015) 107–113.
[9] Nimitha S. Prabhu, Vinod Hegde, M.I. Sayyed, E. Şakar, Sudha D. Kamath, Investigations on the physical, structural, optical and photoluminescence behavior of Er3+ ions in lithium zinc fluoroborate glass system, Infrared Phys. Technol. 98 (2019) 7–15.
[10] D.K. Gaikwad, M.I. Sayyed, S.N. Botewad, Shamsan S. Obaid, Z.Y. Khattari, U.P. Gawai, Feras Afaneh, M.D. Shirshat, P.P. Pawar, Physical, structural, optical investigation and shielding features of tungsten bismuth tellurite based glasses, J. Non-Cryst. Solids 503–504 (2019) 158–168.
[11] S. Dai, J. Wu, J. Zhang, G. Wang, Z. Jiang, The spectroscopic properties of Er3+-doped TeO_2-Nb_2O_5 glasses with high mechanical strength performance, Spectrochim. Acta Part A Mol. Biomol. Spectrosc. 62 (2005) 431–437.
[12] N.S. Tagiara, D. Palles, E.D. Simandiras, V. Psycharis, A. Kyritsis, E.I. Kamitsos, Synthesis, thermal and structural properties of pure TeO2 glass and zinc-tellurite glasses, J. Non-Cryst. Solids 457 (2017) 116–125.
[13] Amandeep Sharma, M.I. Sayyed, O. Agar, H.O. Tekin, Simulation of shielding parameters for TeO_2-WO_3-GeO_2 glasses using FLUKA code, Results in Physics 13 (2019) 102199.
[14] O. Agar, E. Kavaz, E.E. Altunsoy, O. Kilicoglu, H.O. Tekin, M.I. Sayyed, T.T. Erguzel, Nevzat Tarhan, Er_2O_3 effects on photon and neutron shielding properties of TeO_2-Li_2O-$ZnONb_2O_5$ glass system, Results in Physics 13 (2019) 102277.
[15] M. Kurudirek, N. Chutithanapanon, R. Laopaiboon, C. Yenchai, C. Bootjomchai, Effect of Bi_2O_3 on gamma ray shielding and structural properties of borosilicate glasses recycled from high pressure sodium lamp glass, J. Alloy. Comp. 745 (2018) 355–364.
[16] Murat Kurudirek, Yüksel Özdemir, Önder Simsek, Rıdvan Durak, Comparison of some lead and non-lead based glass systems, standard shielding concretes and commercial window glasses in terms of shielding parameters in the energy region of 1 keV–100 GeV: a comparative study, J. Nucl. Mater. 407 (2010) 110–115.
[17] Mridula Dogra, K.J. Singh, Kulwinder Kaur, Vikas Anand, Parminder Kaur, Prabhjot Singh, B.S. Bajwa, Investigation of gamma ray shielding, structural and dissolution rate properties of Bi_2O_3-BaO-B_2O_3-Na_2O glass system, Radiat. Phys. Chem. 144 (2018) 171–179.
[18] Ashok Kumar, M.I. Sayyed, Mengge Dong, Xiangxin Xue, Effect of PbO on the shielding behavior of ZnO–P_2O_5 glass system using Monte Carlo simulation, J. Non-Cryst. Solids 481 (2018) 604–607.
[19] M. Mariyappan, K. Marimuthu, M.I. Sayyed, M.G. Dong, U. Kara, Effect Bi_2O_3 on the physical, structural and radiation shielding properties of Er3+ ions doped bismuth sodiumfluoroborate glasses, J. Non-Cryst. Solids 499 (2018) 75–85.
[20] Marltan Wilson, Optimization of the radiation shielding capabilities of bismuth-borate glasses using the genetic algorithm, Mater. Chem. Phys. 224 (2019) 238–245.
[21] M.I. Sayyed, Kawa M. Kaky, Erdem Şakar, Uğur Akbaba, Malaa M. Taki, O. Agar, Gamma radiation shielding investigations for selected germanate glasses, J. Non-Cryst. Solids 512 (2019) 33–40.
[22] A.E. Ersundu, M. Büyükyıldız, M. Çelikbilek Ersundu, E. Şakar, M. Kurudirek, The heavy metal oxide glasses within the WO_3-MoO_3-TeO_2 system to investigate the shielding properties of radiation applications, Prog. Nucl. Energy 104 (2018) 280–287.
[23] M.K. Halimah, A. Azuraida, M. Ishak, L. Hasnimulyati, Influence of bismuth oxide on gamma radiation shielding properties of borotellurite glass, J. Non-Cryst. Solids 512 (2019) 140–147.
[24] M.I. Sayyed, Half value layer, mean free path and exposure buildup factor for tellurite glasses with different oxide compositions, J. Alloy. Comp. 695 (2017) 3191–3197.
[25] Huseyin Ozan Tekin, M.I. Sayyed, Tugba Manici, Elif Ebru Altunsoy, Photon shielding characterizations of bismuth modified borate esilicateetellurite glasses using MCNPX Monte Carlo code, Mater. Chem. Phys. 211 (2018) 9–16.
[26] D.K. Gaikwad, Shamsan S. Obaid, M.I. Sayyed, R.R. Bhosale, V.V. Awasarmol, Ashok Kumar, M.D. Shirsat, P.P. Pawar, Comparative study of gamma ray shielding competence of WO_3-TeO_2-PbO glass system to different glasses and concretes, Mater. Chem. Phys. 213 (2018) 508–517.
[27] M.I. Sayyed, Saleem I. Qashou, Z.Y. Khattari, Radiation shielding competence of newly developed TeO_2-WO_3 glasses, J. Alloy. Comp. 696 (2017) 632–638.
[28] P. Vani, G. Vinitha, M.I. Sayyed, B.O. Elbashir, N. Manikandan, Investigation on structural, optical, thermal and gamma photon shielding properties of zinc and barium doped fluorotellurite glasses, J. Non-Cryst. Solids 511 (2019) 194–200.
[29] Helena Ticha, Jiri Schwarz, Ladislav Tichy, The structural arrangement and the optical band gap in certain Quaternary PbO–ZnO–TeO_2–B_2O_3 glasses, J. Non-Cryst. Solids 489 (2018) 40–44.
[30] Y.J. Cha, J.H. Kim, J.-H. Yoon, B.S. Lee, S. Choi, K.S. Hong, E.D. Jeong, T. Komatsu, H.G. Kim, Synthesis, electronic polarizability and β-BaB_2O_4 crystallization in BaO–B_2O_3–TeO_2 glasses, J. Non-Cryst. Solids 429 (2015) 143–147.
[31] Petr Mošner, Kateřina Vosejpková, Ladislav Koudelka, Lionel Montagne, Revel Bertrand, Structure and properties of glasses in ZnO–P_2O_5–TeO_2 system, J. Non-Cryst. Solids 357 (2011) 2648–2652.
[32] O. Agar, M.I. Sayyed, F. Akman, H.O. Tekin, M.R. Kaçal, An extensive investigation on gamma ray shielding features of Pd/Ag based alloys, Nuclear Eng. Technol. 51 (2019) 853–859.
[33] L. Gerward, N. Guilbert, K.B. Jensen, H. Levring, WinXCom—a program for

calculating X-ray attenuation coefficients, Radiat. Phys. Chem. 71 (2004) 653–654.
[34] L. Shamshad, G. Rooh, P. Limkitjaroenporn, N. Srisittipokakun, W. Chaiphaksa, H.J. Kim, J. Kaewkhao, A comparative study of gadolinium based oxide and oxyfluoride glasses as low energy radiation shielding materials, Prog. Nucl. Energy 97 (2017) 53–59.
[35] R. El-Mallawany, M.I. Sayyed, M.G. Dong, Y.S. Rammah, Simulation of radiation shielding properties of glasses contain PbO, Radiat. Phys. Chem. 151 (2018) 239–252.
[36] Parminder Kaur, K.J. Singh, Sonika Thakur, Prabhjot Singh, B.S. Bajwa, Investigation of bismuth borate glass system modified with barium for structural and gamma-ray shielding properties, Spectrochim. Acta Mol. Biomol. Spectrosc. 206 (2019) 367–377.
[37] P. Fuochi, U. Corda, M. Lavalle, A. Kovacs, M. Baranyai, A. Mejri, K. arah, Dosimetric properties of gamma and electron-irradiated commercial window glasses, Nukleonika 54 (2009) 39–43.
[38] R. Bagheri, A.K. Moghaddam, S.P. Shirmardi, B. Azadbakht, M. Salehi, Determination of gamma-ray shielding properties for silicate glasses containing Bi_2O_3, PbO, and BaO, J. Non-Cryst. Solids 479 (2018) 62–71.
[39] F. Akman, M.R. Kaçal, M.I. Sayyed, H.A. Karatas, Study of gamma radiation attenuation properties of some selected ternary alloys, J. Alloy. Comp. 782 (2019) 315–322.
[40] I.I. Bashter, Calculation of radiation attenuation coefficients for shielding concretes, Ann. Nucl. Energy 24 (1997) 1389–1401.
[41] B. Speit, Radiation-shielding Glasses Providing Safety against Electrical Discharge and Being Resistant to Discoloration, 1991 (Google Patents).